

## Determination of the recharge area and salinization degree of karst springs in the Lamas Basin (Turkey)

GALIP YÜCE\*

Department of Geological Engineering, Faculty of Engineering-Architecture, Eskisehir Osmangazi University, 26040 Meselik-Eskisehir, Turkey

(Received 21 July 2003; in final form 23 May 2005)

The Lamas Basin is an area covering  $\sim 4400 \text{ km}^2$  situated on the eastern Mediterranean coast of Turkey covered with highly karstified limestone and dolomitic limestone from the Miocene and Mesozoic age, respectively. Owing to the area's low karstification basement, groundwater in the karst aquifer circulates deep from the surface towards the springs along the coast as well as to the submarine springs.

This study aims working out the salinization level and recharge characteristics of the Lamas Basin using environmental isotopes techniques. In the study, the data collected previously to discover, in general terms, the groundwater characteristics within the area are reanalyzed to fulfil the purpose of the study.

In conclusion, it is found that the down gradient karst springs discharging along the Mediterranean coast mostly contain groundwater contributions from higher altitudes with depleted  $\delta^{18}\text{O}$  and  $\delta^2\text{H}$  compositions. The  $\delta^{18}\text{O}$ -altitude effect was determined as approximately  $-0.12\text{‰}/100 \text{ m}$  which may indicate sea-spray intrusion towards inland. As a result, the salinization level of coastal springs changes ranging between 1.2% and 17.0%. Owing to the seawater encroachment,  $\text{Ca-HCO}_3$  water type changes to  $\text{Na-HCO}_3$  or  $\text{Na-Cl}$  water by the cation exchange during the dry period. As the unique freshwater potential extends along the coastal area, the groundwater production should be exploited in a way that seawater encroachment is kept at minimum.

*Keywords:* Hydrogen-2; Hydrogen-3; Karst aquifer; Lamas Basin; Oxygen-18; Salinization; Springs

### 1. Introduction

The Lamas region in Turkey covering an area of  $\sim 4400 \text{ km}^2$  is located between the Taurus Mountains and the Mediterranean Sea with an elevation varying from 0 to 2000 m. The study area is intensively karstified and most of the springs discharge to the coastline. The recharge area of the Lamas region has no sufficient water. Increasing urbanization is the main escalating problem in the area and a major cause of water deficiency. In particular, the water demand during the summer months is continuously increasing. As groundwater is in deep circulation at high altitudes, it is a major problem for people to access freshwater by drilling. Therefore, an in-depth investigation and field research are necessary in the region to reach the

---

\*Tel.: +90-222-239-3750 or 3406; Fax: +90-222-239-3613; Email: gyuce@ogu.edu.tr or galip61@ttnet.net.tr

freshwater wells. In this respect, Önhon *et al.* [1] conducted a study to determine the best well sites for groundwater exploration.

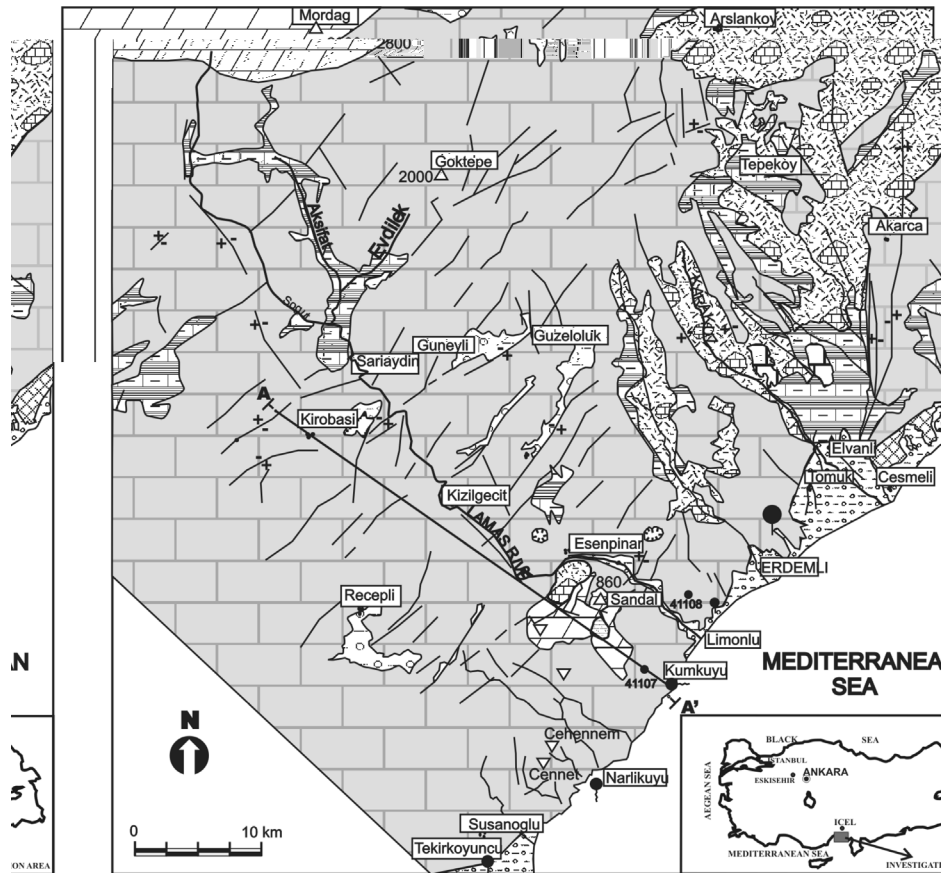
According to the previous studies [1, 2], the geological and hydrogeological frameworks of the area are as follows. The oldest unit in the area is Devonian quartzite (figure 1). It is unconformably overlain by the karstified Mesozoic dolomitic limestones. The Miocene formations, Kaplankaya intercalating with marls, clayey sandy limestone, sandstone, siltstone and Karaisali intensively karstified limestone, are transitional with each other. The alluvium mainly composing of silt, sand and gravel is spread out in the coastal area with a maximum depth of 50 m. The Ophiolitic mélange observed in the east and north of Esenpinar is a complex of limestone, sandstone, siltstone and claystone blocks. The intensive fracture and fault systems developed in Karaisali limestone have accelerated the karstification because Kaplankaya formation acted as impervious layer.

The mean annual precipitation is 756.5 mm in Guzeloluk (1400 m a.s.l.) and 673 mm in Kirobasi (1400 m a.s.l.). On the coastal area, the mean annual rainfall is 605.2 mm in Erdemli (9 m a.s.l.) (figure 2). The karst morphology is very well developed; numerous sinkholes, karst springs, and collapsing dolines characterize the basin. The infiltration from precipitation and runoff has resulted in the karstification which reaches below the sea level at the coastal area. Many karst springs discharge in the area. One of them, K-14, is the main karstic outlet. This spring has an average discharge of  $1.3 \text{ m}^3 \text{ s}^{-1}$  and a minimum discharge of  $0.45 \text{ m}^3 \text{ s}^{-1}$ . Its catchment area covers  $108 \text{ km}^2$ . On the basis of the data, the average annual runoff coefficient is 0.5, which indicates intensive infiltration rates of precipitation (30–40 %) with 10–20 % evaporation. This is identical to the karst catchments under Mediterranean climatic conditions [3].

General hydrogeological properties of the formations are given in figure 3 [4, 5]. The groundwater flows southwards through channels, caverns or fracture and joint systems down to 0 m elevation or to the discharge points as karst springs and submarine springs. The short information about the main springs are as follows: K-2 (Dedekavak spring) is one of the most important springs of the basin and discharges  $\sim 2 \text{ m}^3 \text{ s}^{-1}$  average. K-3 (Erdemli spring) discharges from limestone–alluvium contact from five different points. The measured mean discharge is  $2.1 \text{ m}^3 \text{ s}^{-1}$ , where  $1 \text{ m}^3 \text{ s}^{-1}$  is pumped for irrigation. The mean discharge of K-4 (Karasu spring) is  $0.042 \text{ m}^3 \text{ s}^{-1}$ . K-14 (Susanoglu spring) is a karstic spring discharging from Miocene–Alluvium contact. According to the observations made between 1977 and 1982, the minimum yield was  $0.442 \text{ m}^3 \text{ s}^{-1}$  and maximum was  $2.055 \text{ m}^3 \text{ s}^{-1}$ . K-16 (Kumkuyu spring) is one of the best discharge observation points from Miocene limestone is located on the coastline. Approximately  $0.2 \text{ m}^3 \text{ s}^{-1}$  of water from nearly 0.5 m elevation is pumped for irrigation. According to the measurements in K-19 (Tekir koyuncu spring) made between 1979 and 1991, the minimum yield was 0.026 and  $2.189 \text{ m}^3 \text{ s}^{-1}$ . K-25 (Narlikuyu) spring also discharges from Miocene limestone on the coastline with the mean  $0.050 \text{ m}^3 \text{ s}^{-1}$  yield.

The wells in the region were drilled along the coastline to supply groundwater for agriculture and domestic uses. The transmissivity values are provided from pumping tests reaching up to  $2500 \text{ m}^3$  per day whereas, some wells are completely non-productive due to the preferable pathways of the karst aquifer.

Deep well DSI (State Hydraulic Works) 41107 (figure 2) was drilled to the north of the K-25 spring and south of a sinkhole. The depth of the well is 202.5 m, and the bottom exceeds 56 m below the sea level. The water level is at 146 m that means it is almost at the level of the sea surface. Another deep well, DSI 41108, was drilled on the west bank of the Lamas River, east of the K-4 spring. Despite the fact that the depth of this well is 257.8 m, exceeding 7.8 m below the spring elevation and 37.8 m below the sea level, no water level was detected. The rapid increase of topography at a short distance and effective seawater encroachment into the karst



**EXPLANATIONS**

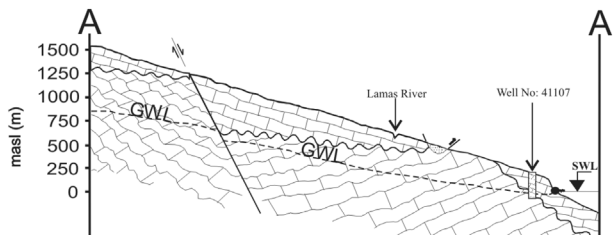
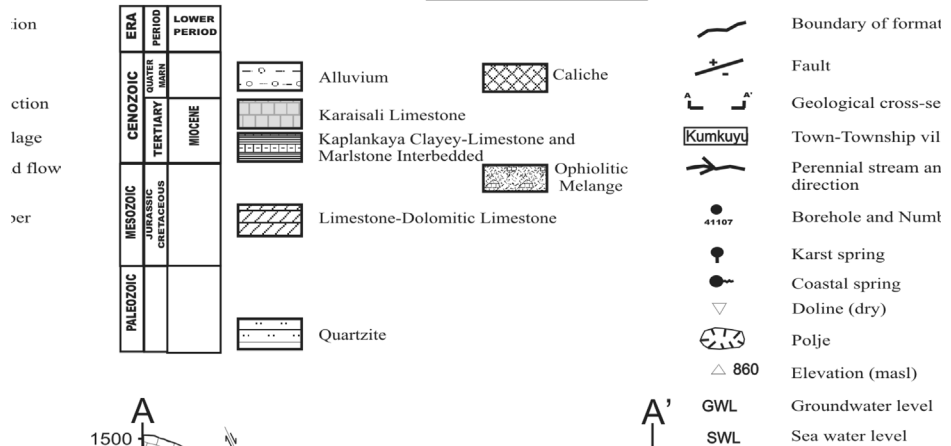


Figure 1. Hydrogeological map of the investigation area (modified from ref. [4]).

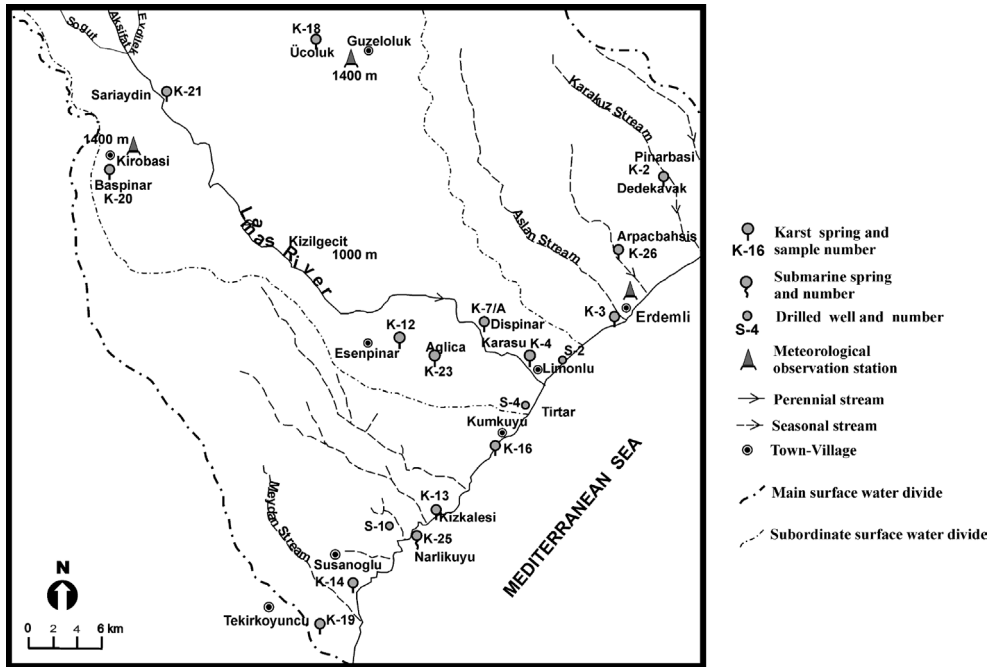


Figure 2. Sampling points in the Lamas Basin (modified from ref. [4]).

system cause difficulties in deep-well drillings for freshwater. This shows that new wells which will be productive are needed to be drilled on the coastline. This brings in a new problem, that is, the effect of the seawater encroachment which is said to be observed clearly in isotopic analyses [1]. However, the evaluation of previous data [1] seems not to be satisfactory to explain the distribution of salinization level and the interrelations of water sources in the area. As it is necessary to apply measures to prevent the seawater encroachment in the settlement area, a detailed evaluation of the salinization levels gains importance. Thus, the aim of this

ERA	PERIOD	STRATIGRAPHY	LITHOLOGY	PHYSICAL PROPERTIES	HYDROGEOLOGICAL PROPERTIES
CENEZOIC	LOWER PERIOD	Holo cene	Alluvium	Sand, gravel	Groundwater bearing
	TERTIARY	MIOCENE	Karaisali Formation Kaplankaya Formation Unconformity	White, dirty, intensively fractured, karstified limestone Base conglomerate, clayey, higher carbonate ratio in upper levels	Aquifer good quality, groundwater in karstified zones. Local groundwater
MESOZOIC	CRETACEOUS	UPPER	Melange (Tepekoym Formation) Tectonical Surface	Consists carbonate rocks, sandstone and claystone blocks	Impermeable
	JURASSIC		Demirkazik Formation Unconformity	Hard, brittle, grey to dark grey, folded and fractured, thick layered	Local groundwater
PALEOZOIC			Quartzite	Red to orange colour, hard and massive	Impermeable

Figure 3. General hydrogeological properties of the formations (modified from ref. [4]).

article is to re-evaluate the data of Önhon's study [1] to work out the degree of salinization and discharge–recharge characteristics of the basin on the basis of available water chemistry and isotope data.

## 2. Methodology

In this study, the stable isotope ratios of oxygen ( $^{18}\text{O}/^{16}\text{O}$ ) and hydrogen ( $^2\text{H}/\text{H}$ ), as well as the radioactive isotope of hydrogen, tritium ( $^3\text{H}$ ), were used. The database of this study was obtained as follows. During 1990 and 1992, 15 karst springs, 3-drilled deep wells and 2 precipitation stations were sampled (figure 2). Throughout the first year, sampling was performed at a monthly interval both for groundwater and precipitation, the second year it was continued on a quarterly for groundwater but monthly for precipitation. The samples from drilled wells were taken after the pumping of wells for 15–20 min, approximately reaching two volumes of the well.

Samples were delivered on the same day to the Laboratory of State Hydraulic Works (DSI) in Ankara for chemical analyses. Water temperature, pH and specific electrical conductivity (EC) were measured *in situ* by Schott-Geräte handy lab model instrument with  $\pm 0.5\%$  for EC and  $\pm 0.1$  for pH reading limits. Water samples were collected into 1000 ml polyethylene containers. Deuterium and oxygen-18 contents were determined by mass spectrometry with an overall precision of 1‰ and 0.1‰, respectively, whereas tritium was measured by liquid scintillation counting of water previously enriched by electrolysis. These concentrations are expressed as TU and errors of measurement  $\pm 1$  are quoted for each tritium value. The values of stable isotopes are expressed conventionally in delta ( $\delta$ ) notation as per mil deviation from the V-SMOW (Vienna Standard Mean Ocean Water). Oxygen-18, deuterium and tritium analyses were carried out at the Technical Research and Quality Control Department of DSI in Ankara.

The stable isotope contents of water samples collected from sampling points, which are under the effect of seawater encroachment, together with the chlorine contents, are used in the correction of isotope values. Thus, the salinization levels are re-calculated using the formula below [6, 7]:

$$f\text{Cl}_{\text{sw}} + (1 - f)\text{Cl}_{\text{fw}} = \text{Cl}_{\text{mix}} \quad (1)$$

$$f = \frac{\text{Cl}_{\text{mix}} - \text{Cl}_{\text{fw}}}{\text{Cl}_{\text{sw}} - \text{Cl}_{\text{fw}}}, \quad (2)$$

where  $f$  is the mixing ratio,  $\text{Cl}_{\text{sw}}$  the seawater,  $\text{Cl}_{\text{fw}}$  the freshwater, and  $\text{Cl}_{\text{mix}}$  the mixing water.

It should be noted that this formula is relevant to the calculation of both chlorine and  $\delta^{18}\text{O}$ . Besides, the precipitation samples, collected from May 1990 to November 1992 from the Guzeloluk Observation Station (1400 m a.s.l.) and from February 1991 to October 1992 from the Erdemli Observation Station (9 m a.s.l.) (table 1), were re-drawn in the graphs and re-evaluated to shed light on the recharge features and salinization issue of the area.

## 3. Results and discussion

The stable isotope concentrations of precipitation were compared in the  $\delta^{18}\text{O}$  vs.  $\delta^2\text{H}$  graph (figure 4) to analyze the isotopic composition with regard to the global meteoric water line (GMWL) and Eastern Mediterranean water line (EMWL).

Table 1. Isotope data of the Erdemli and Guzeloluk precipitation (modified from ref. [1]).

Year	Month	Precipitation (mm)		$\delta^{18}\text{O}\%$		$\delta^2\text{H}\%$		$^3\text{H}$ (TU)	
		Güzeloluk	Erdemli	Güzeloluk	Erdemli	Güzeloluk	Erdemli	Güzeloluk	Erdemli
1990									
	May	78	–	–8.0	–	–51.6	–	18	–
	June	18.8	–	–4.0	–	–23.3	–	24	–
	July	28	–	–8.4	–	–61.0	–	7	–
	September	11.9	–	–2.6	–	–9.2	–	–	–
	October	35.3	–	–6.8	–	–39.9	–	20	–
	November	17.5	–	–8.1	–	–42.0	–	–	–
	December	69.2	–	–6.4	–	–27.4	–	23	–
1991									
	January	54.3	–	–11.7	–	–78.1	–	6	–
	February	64.6	73.8	–9.2	–5.4	–56.0	–34.9	14	21
	March	22	32.3	–7.2	–5.6	–40.6	–39.5	14	47
	April	58.5	54.2	–9.2	–8.1	–64.2	–56.2	14	12
	May	28.4	3.8	–2.7	–3.7	–2.8	–21.5	7	–
	June	12.9	–	–4.9	–	–34.4	–	16	–
	July	42	–	–6.0	–	–38.4	–	17	–
	August	31.1	–	–3.2	–	–	–	–	–
	September	12.5	–	–6.1	–	–	–	–	–
	October	30.8	–	–	–	5.1	–	4	–
	November	43.3	47.4	–	–5.2	–58.7	–24.5	4	14
	December	316.6	293.3	–	–9.4	–67.0	–42.2	3	10
1992									
	January	7.7	0.8	–	–8.1	–114.0	–44.0	–	–
	February	51.6	43.6	–	–8.0	–68.1	–	3	5
	March	97.5	35.8	–	–4.8	–	–	3	4
	April	19.5	4	–	–3.3	–59.0	–22.4	–	–
	May	83.7	90.9	–	–5.6	–32.0	–25.0	10	13
	June	53.4	23.8	–	–4.3	–45.8	–19.7	12	–
	July	–	–	–6.2	–	–	–	8	–
	August	–	–	3.4	–	–0.3	–	–	–
	September	–	–	–6.1	–	–	–	–	–
	October	–	–	–3.7	–	–3.5	–	–	–
	November	–	–	–7.7	–	–	–	–	–

The scatter of the data around the local meteoric water line (LMWL) of the Guzeloluk is close to GMWL that has been described by the equation [7]:

$$\delta^2\text{H}_{\text{vsmow}} = 8 \delta^{18}\text{O}_{\text{vsmow}} + 10. \quad (3)$$

Although the Erdemli precipitation is very close to the EMWL, it shows deviation from the EMWL due to evaporation effect, which EMWL has been described as [8, 9]:

$$\delta^2\text{H}_{\text{vsmow}} = 8 \delta^{18}\text{O}_{\text{vsmow}} + 22. \quad (4)$$

The linear regression equations can be obtained from figure 4 as follows:

$$\text{Güzeloluk} \quad \delta^2\text{H} = 7.68 \delta^{18}\text{O} + 11.72 \quad r = 0.96 \quad n = 14 \quad (5)$$

$$\text{Erdemli} \quad \delta^2\text{H} = 5 \delta^{18}\text{O} - 3.68 \quad r = 0.84 \quad n = 10. \quad (6)$$

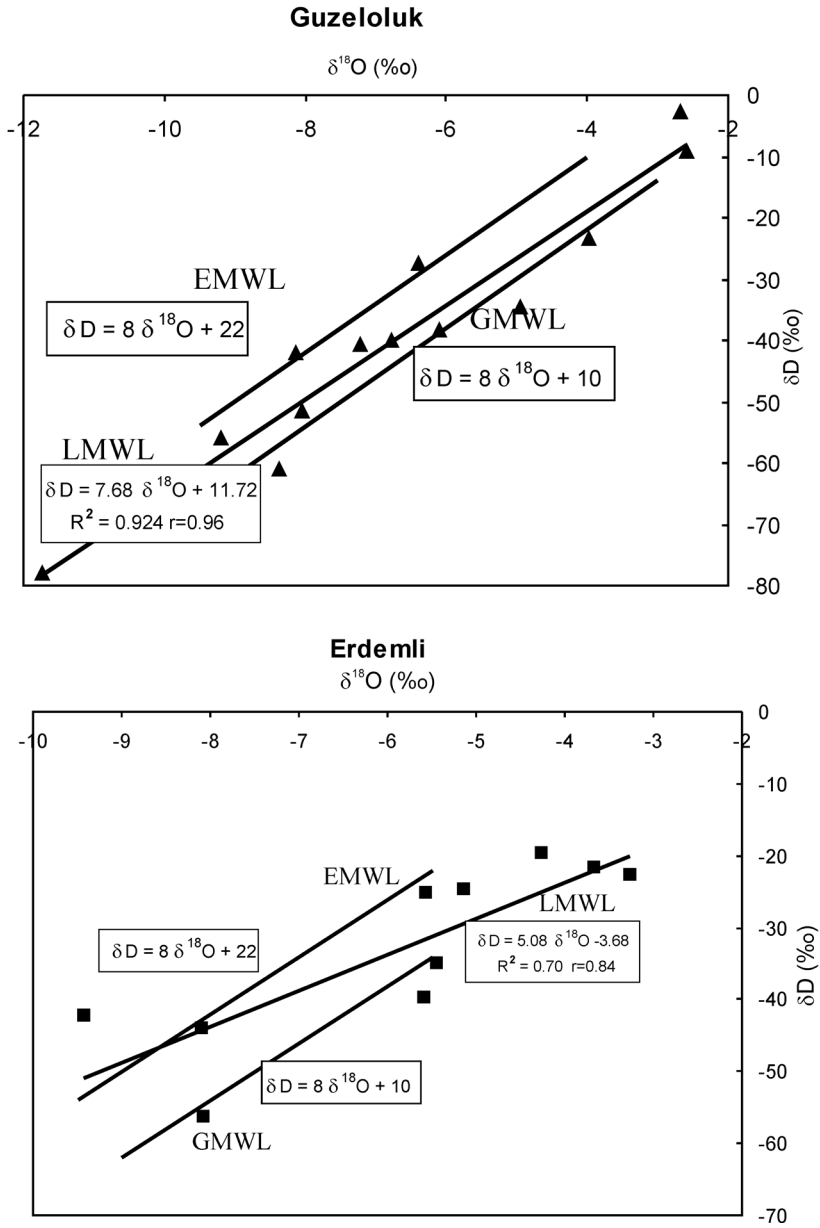


Figure 4.  $\delta^{18}\text{O}/\delta^2\text{H}$  ( $\delta\text{D}$ ) plot for Guzeloluk and Erdemli precipitation.

Relation between  $\delta^{18}\text{O}$  and  $\delta^2\text{H}$  of groundwater (karst springs and deep wells) samples are plotted in figure 5 to determine local groundwater line (LGWL). The plots of the isotopic compositions of groundwater in the study area are generally scattered between GMWL and EMWL, and LGWL is described by the equation subsequently:

$$\delta^2\text{H}_{\text{vsnow}} = 7.79 \delta^{18}\text{O}_{\text{vsnow}} + 14.8. \tag{7}$$

The precipitation values are also plotted in figure 5 for searching relationships with groundwater. Owing to the excess stable isotope value of the Erdemli precipitation that is affected

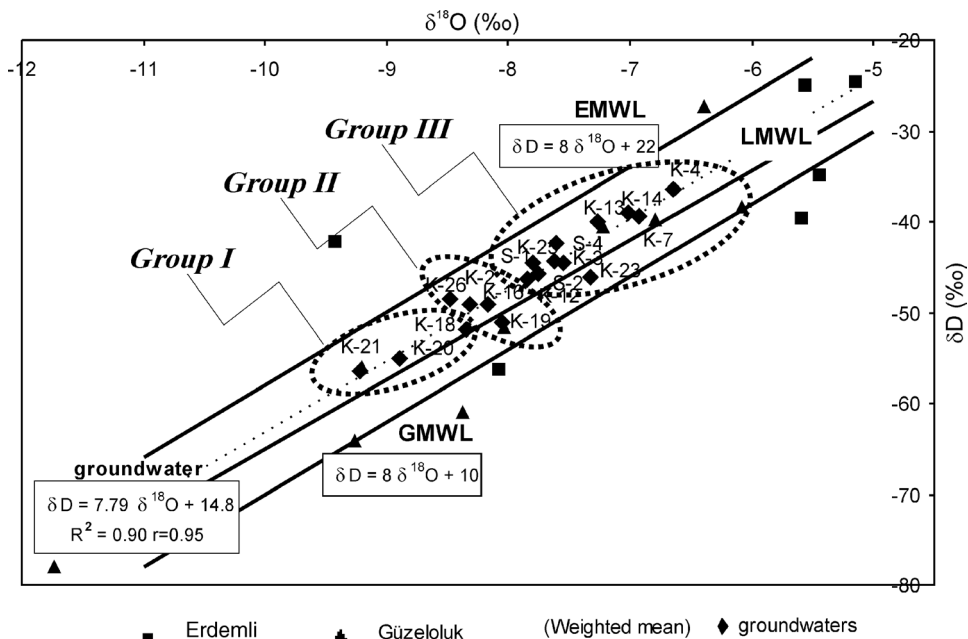


Figure 5. The mean  $\delta^{18}\text{O}/\delta^2\text{H}$  ( $\delta\text{D}$ ) diagram for groundwater of the Lamas region. It is also shown the EMWL, LMWL (Guzeloluk) and GMWL precipitation lines.

by evaporation, the precipitation data belonging to Erdemli station could not be used to indicate groundwater relations. Instead, data of Guzeloluk, as it is seen from the aforementioned discussion and figure 5, can be used: Guzeloluk precipitation values fall in the LGWL which indicates that the groundwater in the area is mostly replenished from precipitation fall in the higher altitudes.

In ref. [1],  $^{18}\text{O}$  and deuterium contents were not evaluated on the  $\delta^{18}\text{O}$  vs.  $\delta^2\text{H}$  graph and the samples were clustered into six groups. This kind of grouping is not satisfactory to evaluate the recharge relations in the area. However, in this study,  $^{18}\text{O}$  and deuterium contents are examined in the  $\delta^{18}\text{O}$  vs.  $\delta^2\text{H}$  graph. As a result (figure 5), the groundwater samples (mostly karst springs) are clustered into three groups around the three meteoric water lines (GMWL, LMWL, and EMWL), which differ from the previous study [1]. These groupings reflect the variation of the recharge conditions [10–12]. Group I refer to the samples that replenished from near the catchment area having slight isotopic depletion. Group II are representative of replenishing from the low-medium altitudes which having relative enrichment isotopically than that of group I. Group III represent the local and the lower altitude recharge with having more isotopic enrichment with respect to group I and group II.

Another examination is the calculation of mean altitude effect. To establish the  $\delta^{18}\text{O}$ -altitude effect for the study area, mainly local outlets with well-defined small catchment areas were selected as reference springs (K-4, K-23, and K-18). The size of the catchment areas of the reference springs range between 0.01 and 0.20  $\text{km}^2$ , defined by map analyses and field work. Thus, by correlating the long-term mean  $^{18}\text{O}$  content and the recharge altitudes of these reference springs the  $\delta^{18}\text{O}$ -altitude effect was determined (table 2 and figure 6). Given the high relief of the study area and, the strong isotopic ( $^{18}\text{O}$ ) variability, the  $\delta^{18}\text{O}$ -altitude effect appeared to be a well-suited tool for determining the mean recharge altitude of the springs. It is figured out that K-20, K-21, K-25 and K-16 are replenished from the highest altitudes of



Table 2. Mean isotope ( $\delta^{18}\text{O}$ ,  $\delta^2\text{H}$ ,  $^3\text{H}$ ), hydrochemical (chloride concentration, EC) and altitude data (modified from ref. [1]).

Sample No	Location	Mean $\delta^{18}\text{O}\text{‰}$	Mean $\delta^2\text{H}\text{‰}$	Mean $^3\text{HTU}$	Mean chloride (ppm)	Altitude (m)	EC ( $\mu\text{ho/cm}$ )	Mean recharge altitudes (m)
K-2	Dedekavak	-8.3	-49.0	8.2	15.0	178	468	1430
	Erdemli	-7.5	-44.6	13.8	21.3	4	509	830
K-4	Karasu	-6.6	-36.4	4	19.4	30	601	30
K-7	Dispinar	-6.9	-39.4	5.2	17.7	110	489	270
K-12	Esenpinar	-7.8	-46.4	13.2	15.0	800	610	1040
K-13	Kizkalesi	-7.3	-40.0	8.3	140.2	0	1022	550
		-7.5 <sup>†</sup>	-40.9 <sup>†</sup>					
K-14	Susanoglu	-7.0	-39.0	6.9	128.4	7	924	400
		-7.1 <sup>†</sup>	-40.6 <sup>†</sup>					
K-16	Kumkuyu	-8.2	-49.2	7.4	248.9	0	1211	1550
		-8.9 <sup>†</sup>	-52.2 <sup>†</sup>					
K-18	Ucoluk	-8.3	-51.9	15.3	11.1	1440	342	1440
K-19	Tekirkoyuncu	-8.0	-51.2	9.5	97.3	7	791	1270
		-8.2 <sup>†</sup>	-52.2 <sup>†</sup>					
K-20	Baspinar	-8.9	-55.1	16.5	9.6	1335	338	1900
K-21	Sariaydin	-9.2	-56.5	19	10.6	1350	383	2180
K-23	Aglica	-7.3	-46.1	9.6	22.6	610	756	610
K-25	Narlikuyu	-7.6	-44.4	3.8	1000	0	3604	1670
		-8.9 <sup>†</sup>	-56.5 <sup>†</sup>					
K-26	Arpacbahsis	-8.5	-48.6	7.3	13.9	150	477	1550
S-1	Ali Kundakci	-7.8	-44.6	4	33.4	60	516	980
S-2	Ali Cadun	-7.8	-45.8	7.2	23.7	4	507	900
S-4	Tirtar	-7.6	-42.5	7	124.7	5	958	960
		-7.8 <sup>†</sup>	-43.3 <sup>†</sup>					
Seawater		1.5		5	8000			

<sup>†</sup>Corrected values for seawater encroachment.

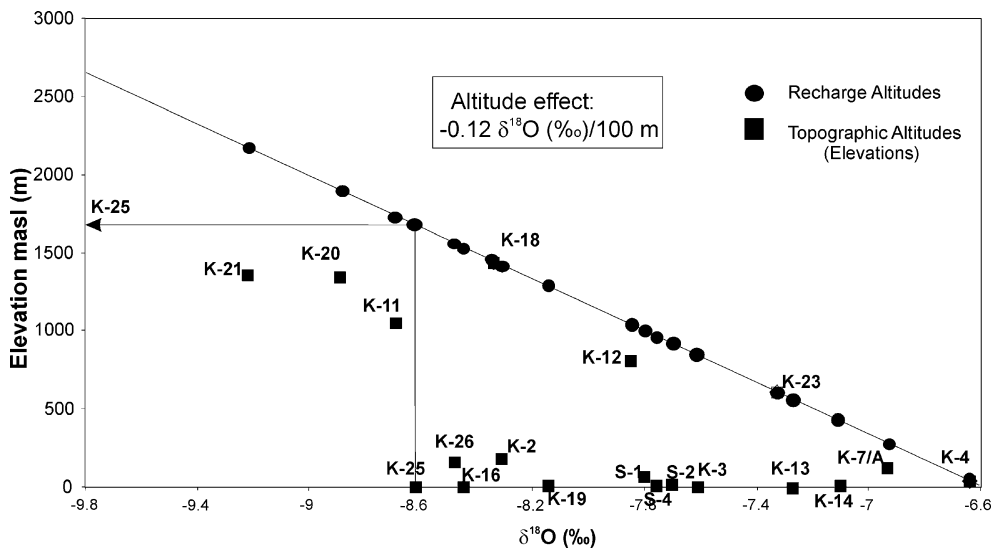


Figure 6. Altitude effect for  $\delta^{18}\text{O}$  values (modified from ref. [1]).

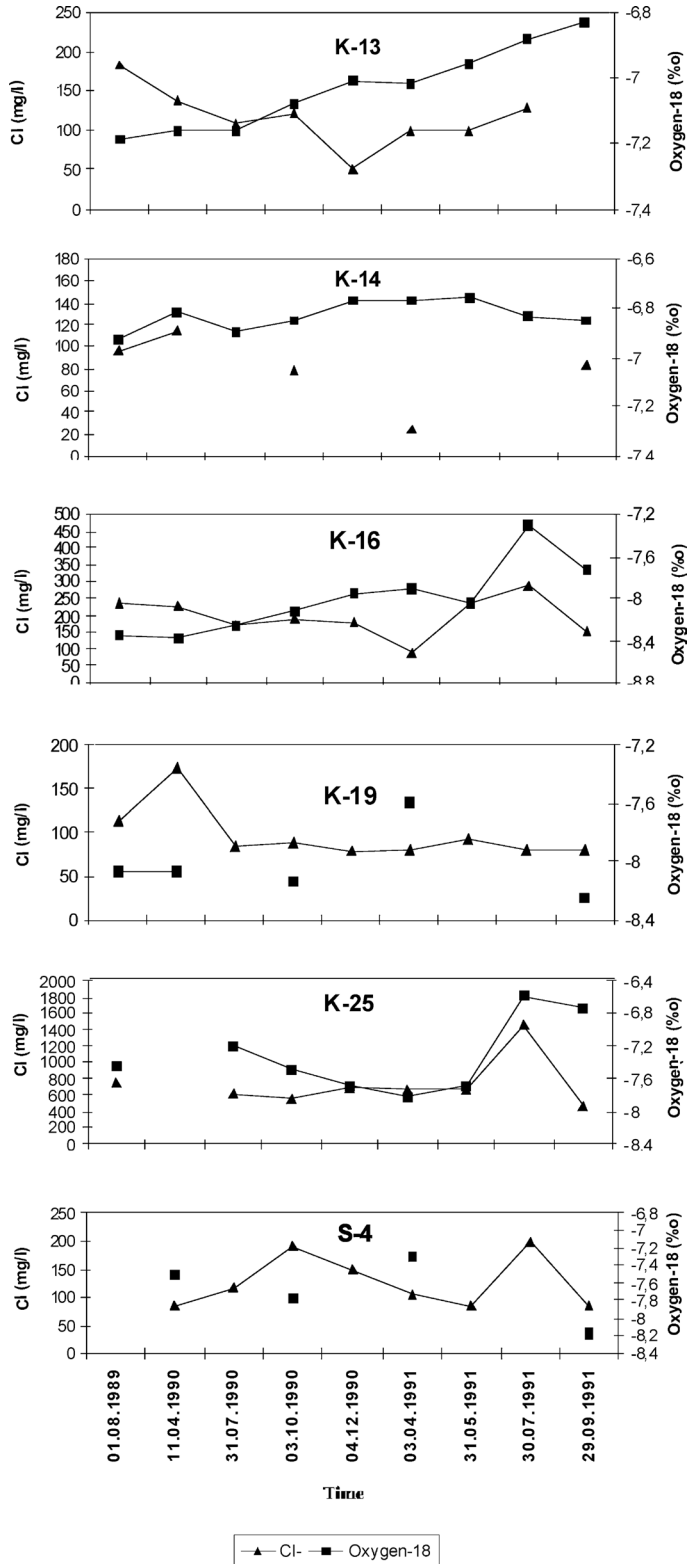


Figure 7. Cl and δ<sup>18</sup>O variations in time.

the catchment area (>1500 m a.s.l.). As a result, the mean altitude effect of  $-0.12\text{‰}/100\text{ m}$  in  $\delta^{18}\text{O}$  is found. This value is lower than the general gradient which varies between  $-0.15$  and  $-0.40\text{‰}/100\text{ m}$  [13]. It may indicate that the coastal precipitation influences the isotopic composition of inland rainfall.

The corrected values for  $\delta^{18}\text{O}$  are given in (\*) mark in table 2. These corrected isotope data were also taken into account for figure 6. The seawater encroachment effects are also observed in  $\text{Cl}^- - \delta^{18}\text{O}$  time series given in figure 7. By examination of the Piper diagram, it can be inferred that during the dry periods, water facies of springs discharging at the coastline (K-13, K-14, K-16, K-19, K-25, and S-4) changes from Ca-Mg-HCO<sub>3</sub> to Na-Cl or mixed water types (figure 8). In studies dealing with seawater intrusion and salinization [6, 11, 14], it is often common to consider both the isotopic and hydrochemical evaluation. The chloride content increases in time depending on groundwater mining. The equilibrium between groundwater and seawater starts to be disturbed by over-pumping in the coastal area of the Lamas Basin. This distortion is escalated by the minimum rainfall replenishment in the dry period. The degree of salinization in the coastal springs based on the end members of mixed solutions vary from

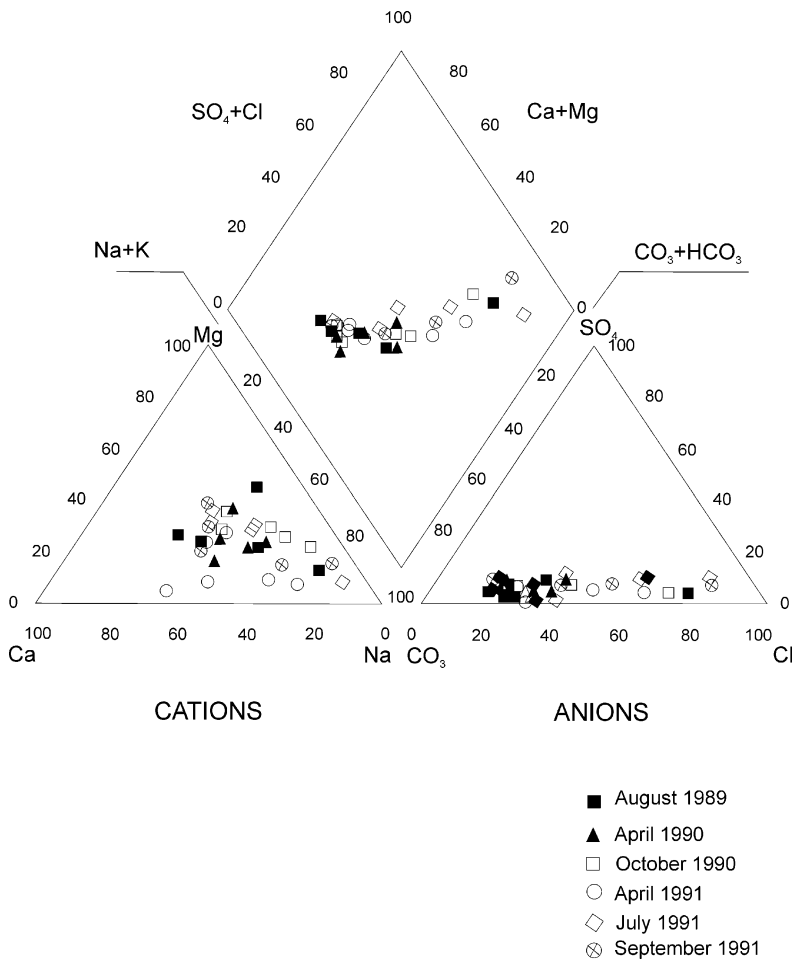


Figure 8. Piper diagram for definition of groundwater chemical types.

1.2 % to 17.0 % for K-19 and K-25, respectively. This salinization degree possibly increases in time unless the over-pumping is stopped. The saline water encroachment might considerably be severe, as the natural hydraulic gradient has been reversed and groundwater is actually moving away from the saltwater–groundwater boundary. Heavy pumping in the coastal area may cause a landward migration of the interface separating fresh and salty groundwater. Thus, the boundary zone will inevitably move much more rapidly because of the high transmissivity of the Karaisali aquifer and saline water will occupy many pores of the aquifer.

The typical relationship of salinity and stable isotope content is shown in figure 9 by plotting  $\delta^{18}\text{O}$ -log  $\text{Cl}^-$ . Three main groups may be noticed in figure 9 in accordance with the  $\delta^{18}\text{O}$  vs.  $\delta^2\text{H}$  graph (figure 5): (1) The group (a) represents low  $\delta^{18}\text{O}$  and  $\text{Cl}^-$  indicating replenishment from high altitudes, (2) the group (b) higher in  $\delta^{18}\text{O}$  and low in  $\text{Cl}^-$  content which reflects the replenishment from medium altitudes, and (3) the group (c) refers to the proportional mixing with seawater.

The relationship between tritium and  $\delta^{18}\text{O}$  values is given in figure 10. Two independent variables,  $\delta^{18}\text{O}$  and  $^3\text{H}$ , represent for replenishment altitudes and residence time of groundwater, respectively [11, 13]. In this respect, waters in group I (K-21, K-20, and K-18) are replenished from the high altitudes (>1400 m a.s.l.) with short residence time. Waters in group II (K-19, K-16, K-26, K-25, and K-2) are fed by the higher altitudes (>1200 m a.s.l.) with the longer residence time (having low-tritium values). Waters in group III (K-13, K-14, K-7, S-1, S-2, S-4, K-23, K-4, K-3, and K-12) are replenished from the medium low altitudes (30 m a.s.l. to 1040 m a.s.l.) with the long residence time. This grouping is in agreement with figure 5.

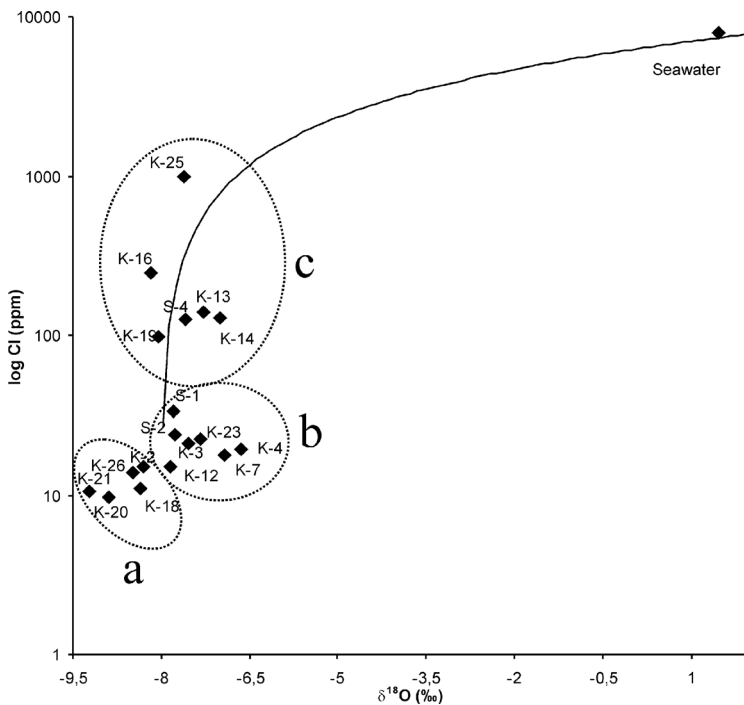


Figure 9. Classification of the sampling points regarding  $\delta^{18}\text{O}$  and  $\text{Cl}^-$  (modified from ref. [6]).

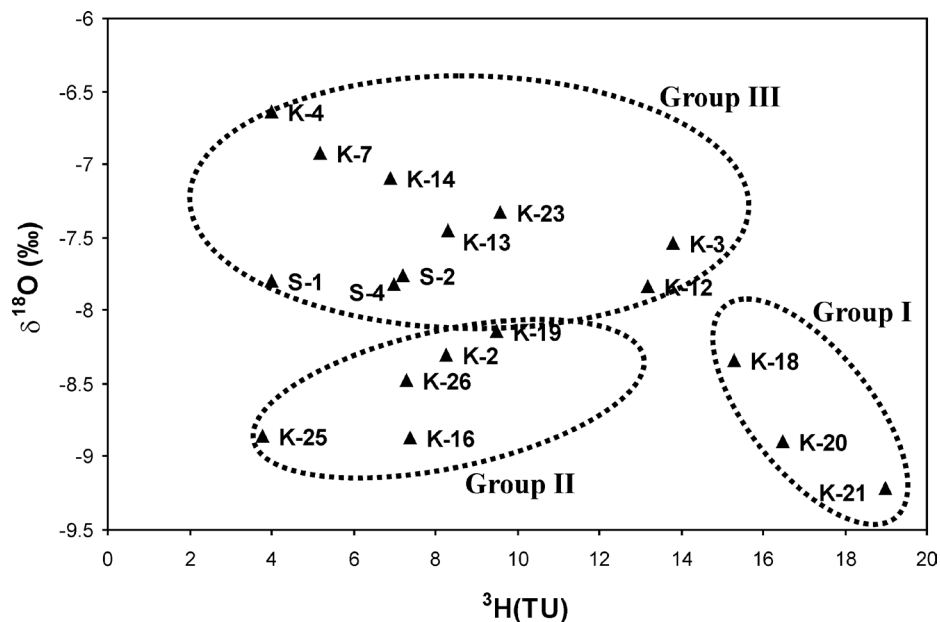


Figure 10. Relationship between  $^3\text{H}$  and  $\delta^{18}\text{O}$  values.

#### 4. Conclusions

The purpose of this article is to enlighten the degree of salinization and the interrelations of water sources in the Lamas Basin. The groundwater in the area is mostly recharged from the high altitudes, whose mean values for  $\delta^{18}\text{O}$  and  $\delta^2\text{H}$  are more depleted. The recharged zone of the karst springs at the coastline is mostly above the altitude of 1200 m a.s.l. The groundwater in the study area is classified as three groups with respect to the replenishing and circulation conditions. Group I (figures 5 and 10) refers to the samples that feed from upstream area. Group II represents replenishing from the low-medium altitudes with the different yields karst springs (varying from  $0.03$  to  $1 \text{ m}^3 \text{ s}^{-1}$ ) discharging to the areas close to the coastline, and group III represents the local recharge. Although the high yield karstic springs are discharged at the coastline, they are fed by the precipitation from higher altitudes rather than local rainfall. This is confirmed by their depleted isotope values. Moreover, these are slightly old waters with low tritium ( $3.8$ – $9.5$  TU) values which are typical for an intensively developed karstified system. The  $\delta^{18}\text{O}$ -altitude effect is determined for all springs in the study area and the mean altitude effect of  $\delta^{18}\text{O}$  is  $-0.12\text{‰}/100 \text{ m}$  which is higher than the general gradient. This indicates the effect of sea spray into inlands.

The most remarkable feature of the coastline springs is the change of  $\text{Ca-HCO}_3$  water at the rainy period towards  $\text{Na-HCO}_3$  or  $\text{Na-Cl}$  water with increased  $\text{Cl}^-$  and  $\text{Na}^+$  concentrations due to seawater encroachment (figures 7 and 8). Indeed, this indicates the cation-exchange process that has been observed in coastal aquifers during replacement of seawater by freshwater of  $\text{Ca-HCO}_3$ ; type with resulting a  $\text{Na-HCO}_3$  water chemistry. The degree of salinization in the coastal springs varies from 1.2 % to 17 % for 1991.

Saltwater encroachment can be prevented by regulating the spacing and withdrawal rates of wells. Depending on the results obtained from this study two suggestions can be made:

1. A dam could be built at high elevations to keep salt water encroachment. This might also recharge to the Karaisali aquifer.
2. To maintain the balance between seawater and freshwater, a line of injection wells could be drilled parallel to the coast which may provide additional freshwater to the aquifer.

### Acknowledgements

This study is based on the research project of General Directorate of State Hydraulic Works (GD-DSI) Project No: TUR/8/011. The author thanks the Geotechnical Services and Groundwater Department, Technical Research and Quality Control Department of GD-DSI for their support during the works and supply of data. Special thanks are given to Mr. Erol Önhon and Mr. Mesut Sayin who generously gave their time to contribute and comment on the manuscript. The initial part of this work was carried out with Dr. Nurettin Pelen. The author is very grateful to Professor Dr. İlknur Keçik and Dr. Halim Mutlu for the linguistic reviews and Didem Uğurluoğlu for the help in editing the manuscript. Earlier version of this manuscript were significantly improved by the comments and suggestions provided by the journal's reviewers.

### References

- [1] E. Önhon, N. Basaran, M. Sayin, D. Can, G. Yüce, N. Pelen. Research on the groundwater flow dynamics of Lamas Basin by isotope methods. DSI–International Atomic Energy Agency Report, pp. 1–53, Ankara, Turkey (1993).
- [2] S. Pampal. Geology of Arslanköy and Tepeköy region in Mersin, Southern Turkey. In *Science Journal*, pp. 247–254, Selcuk University, Konya, Turkey (1984); in Turkish.
- [3] O. Bonacci. Analysis of the maximum discharge of karst springs. *Hydr. J.*, **9**, 328–338 (2001).
- [4] G. Yüce, C. Demirkol. Groundwater potentials of the karst drainage basin in the Lamas Region (Limonlu-Erdemli-Icel). In *Journal of the Engineering Faculty*, pp. 91–117, Adana, Turkey, (1990); in Turkish.
- [5] G. Yüce, N. Pelen, M. Önhon, M. Nazik, T. Karaogullarından, N. Başaran. Karst groundwater studies in Lamas river region (Limonlu-Erdemli-İçel), Turkey. Proceedings of the International Symposium and Field Seminar “Karst Waters and Environmental Impacts”, p. 44, Antalya, Turkey, 10–20 September (1995).
- [6] E. Mazor. *Applied Chemical and Isotopic Groundwater Hydrology*, pp. 139–142, Halsted Press, New York (1991).
- [7] C.A.J. Apello Postma. *Geochemistry, Groundwater and Pollution*, p. 536 Balkema Publisher, Rotterdam (1996).
- [8] H. Craig. Isotopic variations in meteoric waters. *Science*, **133**, 1702–1703 (1961).
- [9] J.R. Gat, I. Carmi. Evolution of the isotopic composition of atmospheric waters in the Mediterranean Sea area. *Geophys. Res.*, **15**, 3039–3048 (1970).
- [10] W.F. Dansgaard. Stable isotopes in precipitation. *Tellus*, **16**, 436–438 (1964).
- [11] I.D. Clark, P. Fritz. *Environmental Isotopes in Hydrogeology*, p. 327, Lewis Publishers, New York (1997).
- [12] S.G. Abd El Samie, M.A. Sadek. Groundwater recharge and flow in the Lower Cretaceous Nubian Sandstone aquifer in the Sinai Peninsula, using isotope techniques and hydrochemistry. *Hydrogeol. J.*, **9**, 378–389 (2001).
- [13] B.T. Verhagen, M.A. Geyh, K. Fröhlich, K. Wirth. *Isotope Hydrological Methods for the Quantitative Evaluation of Groundwater Resources in Arid and Semi-arid Areas: Development of a Methodology*, pp. 8–13, Federal Ministry of Economic Cooperation, Bonn, Germany (1991).
- [14] Y. Yurtsever. Role of environmental isotopes in studies related to salinization processes and salt water intrusion dynamics. In Proceedings of the 13th Salt Water Intrusion Meeting, 5–10 June 1994, G. Barrocu (Ed.), pp. 177–185, Cagliari, Italy (1995).